analytical chemistry

pubs.acs.org/ac Article

Nanostructured Interface Loaded with Chimeric Enzymes for Fluorimetric Quantification of Cyclosporine A and FK506

Paulina K. Wells, Oleh Smutok,* Zhong Guo, Kirill Alexandrov,* and Evgeny Katz*

Cite This: *Anal. Chem.* 2022, 94, 7303−7310 Read Online

ACCESS | Metrics & More | Article Recommendations | Supporting Information

ABSTRACT: Advances in protein engineering resulted in increased efforts to create protein biosensors that can replace instrumentation-heavy analytical and diagnostic methods. Sensitivity, amenability to multiplexing, and manufacturability remain to be among the key issues preventing broad utilization of protein biosensors. Here, we attempt to address these by constructing arrays utilizing protein biosensors based on the artificial allosteric variant of PQQ-glucose dehydrogenase (GDH). We demonstrated that the silica nanoparticle-immobilized GDH protein could be deposited on fiberglass sheets without loss of activity. The particle-associated GDH activity could be monitored using changes in the fluorescence of the commonly used electron mediator phenazine methosulfate. The constructed biosensor arrays of macrocyclic immunosuppressant drugs cyclosporine A and FK-506 displayed very low background and a remarkable dynamic range exceeding 300-fold that resulted in a limit of detection of 2 pM for both analytes. This enabled us to quantify both drugs in human blood, serum, urine, and saliva. The arrays could be stored in dry form and quantitatively imaged using a smartphone camera, demonstrating the method's suitability for field and point-of-care applications. The developed approach provides a generalizable platform for biosensor array development that is compatible with inexpensive and potentially scalable manufacturing.

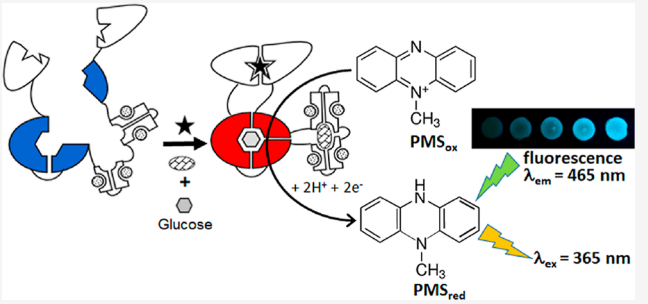

INTRODUCTION

Living systems operate at sub-second scales through the capacity of proteins to selectively bind a large spectrum of molecules and translate such binding events into biochemical activities through allosteric mechanisms. This allosteric regulation process depends on the unique ability of proteins to propagate the impacts of molecular interactions unidirectionally, leading to changes in biological activity. Owing to their switch-like behavior, individual allosteric proteins form intricate networks that transform signals in complex but reproducible ways. Biological systems are therefore able to perform high-order logic operations and respond to their environment rapidly, elastically, and resiliently.[1] Recent years have seen a sustained effort to develop approaches for the construction of artificial protein-based switches with input and output parameters of choice.[2] When intended for sensing applications, these are typically referred to as protein biosensors that can have a variety of architectures and functional mechanisms.[3] While proximity-controlled multicomponent architectures are much easier to construct, they are inevitably influenced by the absolute and relative concentrations of the components. Biosensors composed of a single chain require a much higher level of protein engineering skills in order to integrate both receptor and reporter functionalities within the same polypeptide chain. Initially, the progress in this area came from an approach known as domain insertion where a domain known to undergo a conformational change upon ligand binding is integrated into a reporter domain.[4] Conformational change modulates the activity of the reporter domains generating a quantifiable output. The most widely used implementations of this approach are biosensors based on circular permutated fluorescent proteins.[5] Fluorescent biosensors of neurotransmitters and calcium revolutionized cell and neurobiology by enabling real-time monitoring of neuronal activity.[6] A related approach is based on the detection of conformational change in the receptor domains through a special rearrangement of the fused protein domains from FRET or BRET pairs.[6] These biosensor architectures rely on the availability of receptor domains with conformational changes sufficiently large to modulate the receptor's activity. However, a comprehensive computational analysis of ligand binding domain structures revealed that the large conformational changes are relatively rear, resulting in paucity of suitable receptor domains.[7] Furthermore, most of the single-component biosensors were optimized for a particular class of analytes, and developing protein biosensors that can be

Received: February 8, 2022
Accepted: May 2, 2022
Published: May 11, 2022

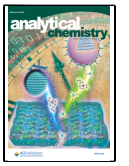

https://doi.org/10.1021/acs.analchem.2c00650
Anal. Chem. 2022, 94, 7303−7310

controlled by both small molecules and large polymers, such as proteins, have not been possible. To overcome this problem, we developed an alternative approach to protein biosensor design where the activity of the reporter is controlled by the level of disorder of artificial N- and C-termini created through circular permutation. Scaffolding of the termini by ligand-controlled dimerization domains reduces the disorder of the termini and increases the activity of the system.[8,9] The former publication reported electrochemical biosensors based on circular permuted PQQ-glucose dehydrogenase. We demonstrated that such biosensors were able to detect both small molecules and protein biomarkers in solution assays with high specificity and limit of detection (LOD) in a mid-pM range. We were able to construct sensory electrodes based on those proteins and demonstrated that they could detect their cognate biomarkers in whole human blood and saliva. While electrochemical detection offers numerous advantages, it also has some drawbacks. One of them is a low potential for multiplexing as this requires development of sophisticated electrodes and fluid-handling systems.[10−12] Unlike electrochemical methods, optical detection technologies allow utilization of spatial and spectral information enabling constructions of sensory arrays—an approach used widely in the construction of DNA-based arrays.[13−15] Electrochemiluminescence[16] has been exploited to convert an electrochemical signal into an optical readout, but its multiplexing still requires a sophisticated electrode design.[17,18] Yet, only some enzymatic reactions are amenable to this approach and, for instance, cannot be easily adopted to PQQ-glucose dehydrogenase (GDH)-based biosensors. Therefore, we sought an alternative approach for converting enzymatic activity of GDH into optically measurable readout. Here, we show that GDH-catalyzed reduction of phenazine methosulfate (PMS) results in the formation of a highly fluorescent product that can be quantified using simple optical setups, such as mobile phone camera. This enabled us to construct biosensor arrays that allow ultrasensitive quantification of small molecules and proteins in biological fluids using simple fiberglass-based biosensor arrays.

EXPERIMENTAL SECTION

Reagents and Materials. Cyclosporine A (CPA) and tacrolimus (FK506) drugs were purchased from Sigma-Aldrich. The calmodulin-binding peptide, M13, skeletal muscle myosin light chain kinase peptide with sequence KRRWKKNFIAVSAANRFKKISSS[19] was purchased from AnaSpec, Fremont, CA, USA. Chimeric CPA- and FK506-activated PQQ-dependent glucose dehydrogenases (CPA-GDH and FK506-GDH) were prepared and characterized according to the procedures detailed in the Supporting Information. Pyrroloquinoline quinone (PQQ), D-(+)-glucose, phenazine methosulfate (PMS), glutaric dialdehyde, 4-(2-hydroxyethyl)-1-piperazineethanesulfonic acid (HEPES buffer), (3-aminopropyl)-triethoxysilane (APTES), and other standard organic and inorganic reagents were purchased from Acros Organics and MilliporeSigma (formerly Sigma-Aldrich). All commercial organic/inorganic chemicals, solvents, and materials were used without further purification.

SiO_2 nanoparticles (SiO_2-NPs; ca. 200 nm) were purchased from Fiber Optics Center Inc. Glass microfiber filter paper 0.5 μm, 90 mm, was obtained from Maine Manufacturing LLC, glass microslides were purchased from VWR, and double-sided mounting tape produced by Scotch was purchased from Walmart.

Biological samples: Serum from human male AB plasma, US origin, sterile-filtered, was purchased from MilliporeSigma. Whole blood was purchased from Zen-Bio Inc., collected from a healthy, Hispanic, 33 year-old male. Urine, saliva, and sweat were collected from a healthy, white, 27 year-old female. Urine was collected in the morning, without prior drinking. Saliva was collected 3 h after a meal; the mouth was rinsed with water prior to collecting. Sweat was collected from the inner part of the wrist after performing high-intensity exercises for 30 min.

All experiments were carried out using ultrapure water (18.2 MΩ·cm; Barnstead Nanopure Diamond) at room temperature (22 ± 2 °C). In some of the experiments, human biofluids with different dilutions were used.

Preparation of Sensor Array. A sensor array was constructed using a glass microscope slide as a support. A VWR glass microscope slide (75 mm × 25 mm × 1.2 mm) was cleaned with ethanol and distilled water prior to its modification. A piece of fiberglass (Maine Manufacturing LLC) was force-adhered to one side of a double-sided tape with the smoother side facing up. A hole-punch tool (office puncher) was used to create fiberglass/tape discs with a diameter of 0.25 inch (6.35 mm). The resulting disc circles attached to the glass microscope slide at even intervals matched to the spread of a multichannel pipette (Figure S1 in the Supporting Information).

Functionalization of SiO_2-NPs and Immobilization of Chimeric Enzymes (CPA-GDH and FK506-GDH). SiO_2-NPs (100 mg) were placed in a plastic tube (Eppendorf) containing 1 mL water with pH adjusted to ca. 9−10, and the suspension was sonicated for 60 min and then centrifuged at 1000 rpm for 10 min at room temperature. Then, the water was replaced with ethanol and centrifuged three more times, changing ethanol each time. APTES (97%, 30 μL) was added to 970 μL of ethanol, and the resulting solution was added to the SiO_2-NPs suspension in ethanol. The mixture was vortexed and left in a shaker (mild shaking) for 3 h. The reacting mixture was centrifuged for 10 min at 10,000 rpm (20 °C), and the liquid supernatant was changed to a 25 mM HEPES buffer, pH 7.4, 1 mL (repeated three times, changing the buffer each time). The suspension of the silanized SiO_2-NPs was mixed with glutaric dialdehyde (0.04% v/v in a 25 mM HEPES buffer, pH 7.4) and slowly shacked with an orbital shaker for 1 h. Then, 5 μL of 25 μM enzyme's preparation (CPA-GDH or FK506-GDH mutants) and 0.5 μM PQQ were added with the next incubation lasted 1 h (in the dark, with slow mixing every 10 min, at room temperature). Then, the formed suspension was washed with 1660 μL of 6 mM HEPES buffer, pH 7.4, and shaking for 1 min (mild mixing) and then centrifuged for 3 min at 1000 rpm. The majority of the supernatant (1660 μL) was collected, and the residual was stored at 8 °C until required.

It should be noted that the enzyme immobilization method based on the use of glutaric dialdehyde provides flexibility for the immobilized enzyme. Indeed, the Schiff base bond formation is a reversible process resulting in bond formation and dissociation. Since the immobilization results in the formation of multiple bonds, the enzyme immobilization is stable, but each individual bond is unstable, thus providing structural flexibility for the immobilized enzyme, which is important for its switchable allosteric function.

https://doi.org/10.1021/acs.analchem.2c00650
Anal. Chem. 2022, 94, 7303−7310

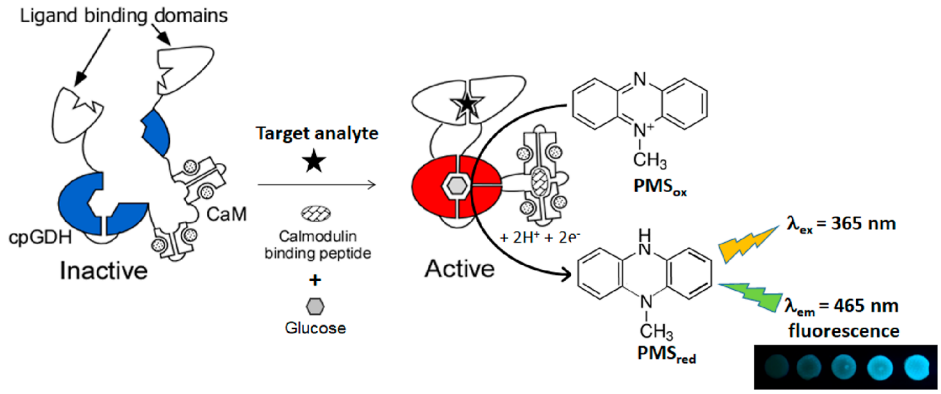

Figure 1. Schematic of the GDH-based biosensor operation with a fluorescence output signal. Used abbreviations: cpGDH—circular permutated; PQQ—glucose dehydrogenase; CaM—calmodulin; and PMS_{ox} and PMS_{red}—phenazine methosulfate reduced and oxidized states, respectively.

Construction of SiO_2-NPs/Chimeric Enzymes' Sensor Array. A SiO_2-NP/chimeric enzyme's suspension (20 μL) was placed on each fiberglass paper-based spot and left for drying at room temperature for 20 min using a hairdryer (low speed, cold air). The sensor plates modified with SiO_2-NP/chimeric enzymes were stored at 8 °C until required.

Activation of the Chimeric Enzymes. Chimeric enzymes (FK506-GDH or CPA-GDH) are not biocatalytically active in their ground state. To be activated, the M13 peptide and a specific analyte such as FK506 or CPA have to bind to the calmodulin (CaM) domain and receptor domains, respectively.[8] After placing SiO_2-NPs with the immobilized enzyme on spots and drying them for 20 min, 20 μL solution of 0.5 μM M13 and variable concentrations of the analyte (FK506 or CPA) were added on each spot in 25 mM HEPES buffer, pH 7.4, also containing 3 mM calcium acetate and 100 mM sodium sulfate. The samples were incubated for 10 min in a fume hood and dried for 20 min using a hairdryer (cold air, low speed).

Sensor's Activity Analysis. To visualize the FK506-GDH or CPA-GDH activity, 20 μL of a reagent solution containing 25 mM HEPES buffer, pH 7.4, with 3 mM calcium acetate, 1 μM PMS, and 20 mM glucose was simultaneously deposited onto each spot of the sensor's array using a multichannel pipette. The enzymatic reaction of glucose consumption (with the simultaneous PMS reduction) was performed for 10 min in the dark at room temperature. Then, the sensor plate was rinsed twice (first by dipping and then by mild shaking for 2 min in 25 mM HEPES buffer, pH 7.4). It was then placed into the UV Fluorescence Analysis Cabinet with a UV lamp operating at a wavelength of 365 nm and a power of 150 μW (Figure S1A in the Supporting Information). A smartphone photo camera was then used in the manual mode (ISO 400; speed 1/15) in order to take photos of the resulting fluorescence. The photo images were converted to a grayscale (black-and-white) format and processed with a standard software ImageJ (Figure S2 in the Supporting Information) to estimate the fluorescence intensity of each sensing spot. The numerical data was then transferred to either Excel or OriginLab, where corresponding graphs were created. The final signal processing steps could be performed with a smartphone or with a regular computer, as convenient.

In order to obtain the apparent K_d of the analyte interaction with the protein biosensor, the fluorescence values for the individual concentrations of the analyte from a single experiment were plotted against the concentration of the ligand, and the data were fitted to the explicit solution of the quadratic equation describing the E + S ↔ ES binding equilibrium, where K_d is defined as $K_d = [E] \times [S]/[EL]$, where $[E_0]$ and $[L_0]$ refer to the total enzyme and ligand concentration (free and bound) on the array. In the fit procedure, the concentration of the biosensors was allowed to vary. Under these conditions, the fluorescence is described by eq 1

$$L = L_{obs(min)} + (L_{obs(max)} - L_{obs(min)}) /(([E_0] + [L_0] + K_d)/2 - ([E_0] + [L_0] + K_d)2/4 - [E_0] \times [L_0])1/2/[L_0] \quad (1)$$

L_{obs} represents the fluorescence, while $L_{obs\ (min)}$ and $L_{obs\ (max)}$ refer to the minimal and maximal fluorescence observed, respectively. A least-squares fit of the data to eq 1 using the software package Grafit 5.0 (Erithacus software) was used to determine the K_d value.

To calculate the dynamic range, we determined the background activity by determining the difference between fluorescence in the absence of the ligand (FK506 or CPA) and in the absence of the ligand and the biosensor. Subsequently, we calculated the maximal signal as the difference in spot-fluorescence between fluorescence at the saturated concentration of ligand (FK506 or CPA) and the spot-fluorescence in the absence of the biosensor. The dynamic range was calculated as the ratio of these two fluorescence values.

The insignificant background fluorescence of the enzyme-modified nano-structured surface could come from fluorescent amino acids (e.g., tryptophan and tyrosine) in the enzyme structure, as well as the optical properties of the SiO_2 nanoparticles under the UV light. The background fluorescence depends on the efficiency of the enzyme immobilization and nanoparticles' load on the highly porous fiberglass support. To exclude the measurement error from the background fluorescence, the two first spots of each sensor plate are used as a blank (with the addition of all reagents except the substrate), and the intensity of all the other spots are analyzed as the fluorescence increase versus the intensity of the blank spots (taken as "0" null).

Using Developed Sensors to Analyze the Biological Fluids Spiked with Cognate Ligands. Biological human fluids (blood, serum, saliva, sweat, and urine) were first diluted for 10, 50, or 100 times (depending on fluid's type) with 20 mM HEPES, pH 7.4, containing 3 mM calcium acetate and

https://doi.org/10.1021/acs.analchem.2c00650
Anal. Chem. 2022, 94, 7303−7310

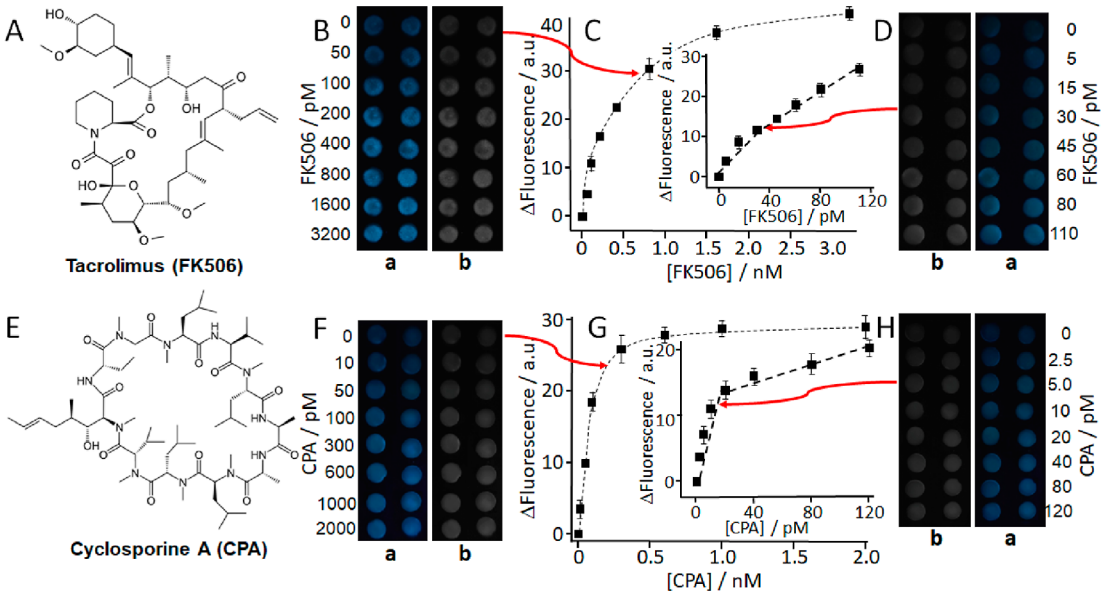

Figure 2. Quantification of tacrolimus (FK506) (A) and cyclosporine A (CPA) (E) using cpGDH biosensors. (B) Fluorescence images obtained with the FK506-GDH-modified spots in the presence of different concentrations (0−3200 pM) of FK506. (C) The fluorescence response measured for different concentrations of FK506. Inset: the fluorescence measured at low concentrations of FK506 (dynamic range: 0−110 pM). (D) Fluorescence images obtained with the FK506-GDH-modified spots in the presence of different concentrations (0−110 pM) of the FK506 analyte. (F) Fluorescence images obtained with the CPA-GDH-modified spots in the presence of different concentrations (0−2000 pM) of the CPA analyte. (G) Fluorescence response measured for different concentrations of CPA. Inset: fluorescence measured at low concentrations of CPA (two dynamic ranges with different slopes: 5−20 and 20−120 pM). (H) Fluorescence images obtained with the CPA-GDH-modified spots in the presence of different concentrations (0−120 pM) of the CPA analyte. Images (a) in (B,D,F,H) correspond to the original photos obtained under UV illumination; (b) images after their conversion to the black-and-white format.

100 mM sodium sulfate. Then, they were spiked with different concentrations of the specific analytes (FK506 or CPA) and 20 mM glucose to achieve its saturating concentration and eliminate the effects of glucose in the sample. The enzyme activation and procedure of sensor's analysis was the same as described above.

Analysis of Sensor Array Stability. To analyze the stability of the sensors, the enzymes (CPA-GDH and FK506-GDH) were immobilized on a fiberglass paper support with the SiO_2-NPs (as described above). The prepared biosensors were placed in a well-sealed Petri dish and stored at +8 °C in a fridge. The biosensors were tested every few days (at day 1, 3, 8, 15, 21, and 61), followed by activation of chimeric enzymes with 0.5 μM M13 and different concentrations of specific ligands (0, 0.1, and 0.5 nM of FK506 for FK506-GDH and CPA for CPA-GDH). The enzymatic activity analysis was performed according to the procedure described before.

RESULTS AND DISCUSSION

The artificial chimeric enzymes based on the PQQ-dependent glucose dehydrogenase (GDH) domain combine three biorecognition units, two responsible for binding a specific target analyte and one for binding the M13 peptide that, when occurring simultaneously, lead to structural rearrangement in the GDH reporter that results in an increased catalytic activity (Figure 1).[8] In other words, the GDH activation occurs only when all recognition units bind their corresponding species such as, for instance, CPA or FK506 macrocyclic compounds and M13 peptide. When the GDH enzyme is activated, its biocatalytic activity can be detected electrochemically (note that GDH is capable of direct, non-mediated, electron transfer to an electrode).[20,21] The biocatalytic reaction can also be monitored following changes in the absorption of electron-accepting dye. Solution assays based on this principle were used extensively to monitor the activity of GDH and thereon based protein biosensors.[22] Here, we tested the utility of the optical detection method for the construction of GDH biosensor arrays. We sought to exploit the fluorescence of the reduced state of the electron mediator phenazine methosulfate (PMS) (λ_{ex} = 365 nm; λ_{em} = 465 nm). Therefore, the biocatalytically generated fluorescence signal was used to follow the GDH activity stimulated by CPA or FK506 analytes in the concentration-dependent fashion (Figure 1). This approach has three major advantages: (i) the high-sensitivity characteristic of fluorescence measurements where even single-photon detection can be achieved with appropriate equipment, (ii) a multiplexed detection mode allowing the construction of arrays for simultaneous measurements of different analytes and different concentrations, and (iii) the measurements performed using a simple smartphone without any sophisticated analytical instrumentation.

To create a biosensor array, we used a nano-structured support composed of fiberglass with deposited SiO_2 nanoparticles (SiO_2-NPs) (Figure S3 in the Supporting Information) that allows immobilization of a large amount of the enzymes (Figure S4 in the Supporting Information) compared to a smooth solid support. The SiO_2-NPs with the immobilized enzymes were visualized using confocal fluorescent microscopy (Figure S5 in the Supporting Information). In the confocal microphotography, enzymatically reduced PMS coloring the fiberglass paper support in a typical blue color is observable from ca. 125 μm inside the supporting fabric to ca. 625 single monolayers of the SiO_2-NPs with immobilized enzymes (taking into account that the average diameter of the SiO_2-NPs is 200 nm). This multilayer formation supports high local fluorescence intensity of the formed dye, significantly

https://doi.org/10.1021/acs.analchem.2c00650
Anal. Chem. 2022, 94, 7303−7310

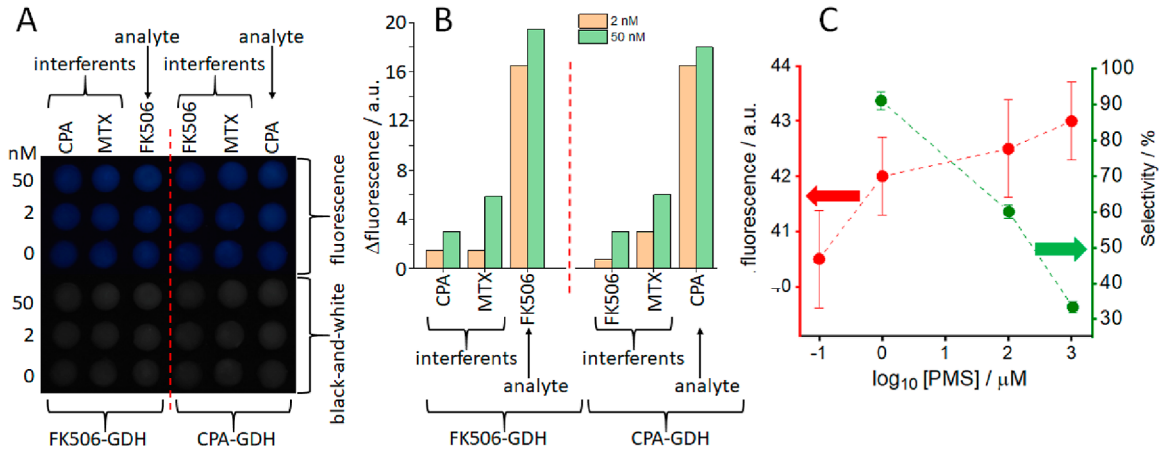

Figure 3. Analysis of sensitivity and selectivity of the biosensor responses measured in the presence of interferents. (A) Images obtained for the fluorescence output measured under UV illumination in the presence of FK506 and CPA analytes with the FK506-GDH and CPA-GDH enzymes, respectively, also using interferents CPA and MTX with the FK506-GDH and interferents FK506 and MTX with CPA-GDH. (B) Analysis of the responses derived from images shown in (A). (C) The biosensor activity (fluorescence increase) and selectivity at different PMS concentrations (FK506-GDH responses to the 2 mM target analyte FK506 in % to the total response in the presence of 2 nM MTX as the interfering sample).

improving the sensitivity of the biosensor. Moreover, the deep penetration of the enzyme-functionalized SiO_2-NPs into the fiberglass paper prevents their wash out, providing high stability of the biocatalytic film.

Prior to the biosensor characterization with different concentrations of the analytes (FK506 and CPA), we studied the time-dependent fluorescence signal appearance for the FK506 measurements using the immobilized FK506-GDH enzyme (Figure S6 in the Supporting Information). This experiment was important to find the time point at which the signal reached saturation (30 min), to be used in all the following experiments. It should be noted that this time is not only for the biocatalytic reaction to proceed but it also includes the time needed for the ligand-induced isomerization of the biosensors resulting in the formation of its active state.[8]

Figure 2 shows the results for the analysis of the biosensor array's response to different concentrations of CPA and FK506. The fluorescent images (blue) were converted to the gray (black-and-white) format, and then the images were digitized by measuring the brightness by counting the pixels in them using the ImageJ software installed in the smartphone (Figure S2 in the Supporting Information). The digitized data was plotted as a function of the fluorescence intensity (after subtraction of the background fluorescence) on the target analyte concentrations. While the absolute concentration of the active biosensors associated with the reaction zones is difficult to quantify, the fit of the data allows estimation of an apparent K_d. Using this approach, we determined K_d constants of ca. 400 ± 30 pM and ca. 80 ± 10 pM for the FK506-GDH and CPA-GDH enzymes, respectively (Figure 2C,G). The obtained K_d values are somewhat lower than those previously obtained using solution assays (0.96 nM for FK506 and 0.28 nM for CPA) but reasonably close and well correlated.[8] The assay, however, demonstrates a very large dynamic range of 310-fold for FK506-GDH and 470-fold for CPA-GDH. This appears to be a consequence of very low background luminescence and the high catalytic activity of GDH-based biosensors. As a result, the obtained limits of detection (2 pM) are significantly lower than those that could be previously achieved in solution assays (50 pM).[8] The response of the FK506-GDH-based array to FK506 was biphasic with the near-linear response between 2−20 and 20−120 pM. A similar behavior was observed in the case of CPA-GDH-based biosensor where the near-linear concentration-dependent responses are 2−15 and 20−120 pM of the CPA analyte. While the nature of biphasic biosensor response is not clear at this point, and was not observed in the solution assays, it has a potential advantage for the analysis of immunosuppressant compounds in the samples of transplant patients, where their concentrations vary widely.

While the detection limits are quite impressive (note that it is very rare to find a sensor with the ability to detect picomolar concentrations of target analyte), the selectivity to the target analytes is highly important, and it was studied in detail (Figure 3). It was found that the sensitivity and selectivity of the drug analysis are changing in the opposite way depending on the PMS concentrations (Figure 3C). Indeed, the analysis of the target analyte (FK506 and CPA) by the corresponding biosensor is not significantly different for the broad range of PMS concentrations: 1−1000 μM. The sensitivity of the systems decreases at lower PMS concentrations (1−0.1 μM). On the other hand, the selectivity versus interferents is significantly decreased with the increase of the PMS concentration (Figure 3C). These experiments allowed us to choose an optimal PMS concentration of 1 μM where the selectivity and sensitivity of the system are well balanced.

In the next step, we used the developed method to quantity FK506 and CPA drugs in biological human fluids: whole blood, serum, saliva, sweat, and urine. Since these complex biological fluids include components that may produce autofluorescence with wavelengths close to that of $PMS_{reduced}$ emission, we analyzed the fluorescence of biofluids using the same bioanalytical platform (Figure S7 in the Supporting Information). The highest fluorescence background was observed in the urine and serum. However, high sensitivity in the developed method allows quantification of the drugs in bodily fluids after their significant dilution. To ascertain the practical utility of the approach, the dilution factors were chosen in keeping with the expected concentrations of analyte drugs in clinical samples (1−30 nM for FK506 and 100−1500 nM for CPA) (Table S1 in the Supporting Information).[23] Figure 4 shows the fluorescent analysis of the analyte drugs in

https://doi.org/10.1021/acs.analchem.2c00650
Anal. Chem. 2022, 94, 7303−7310

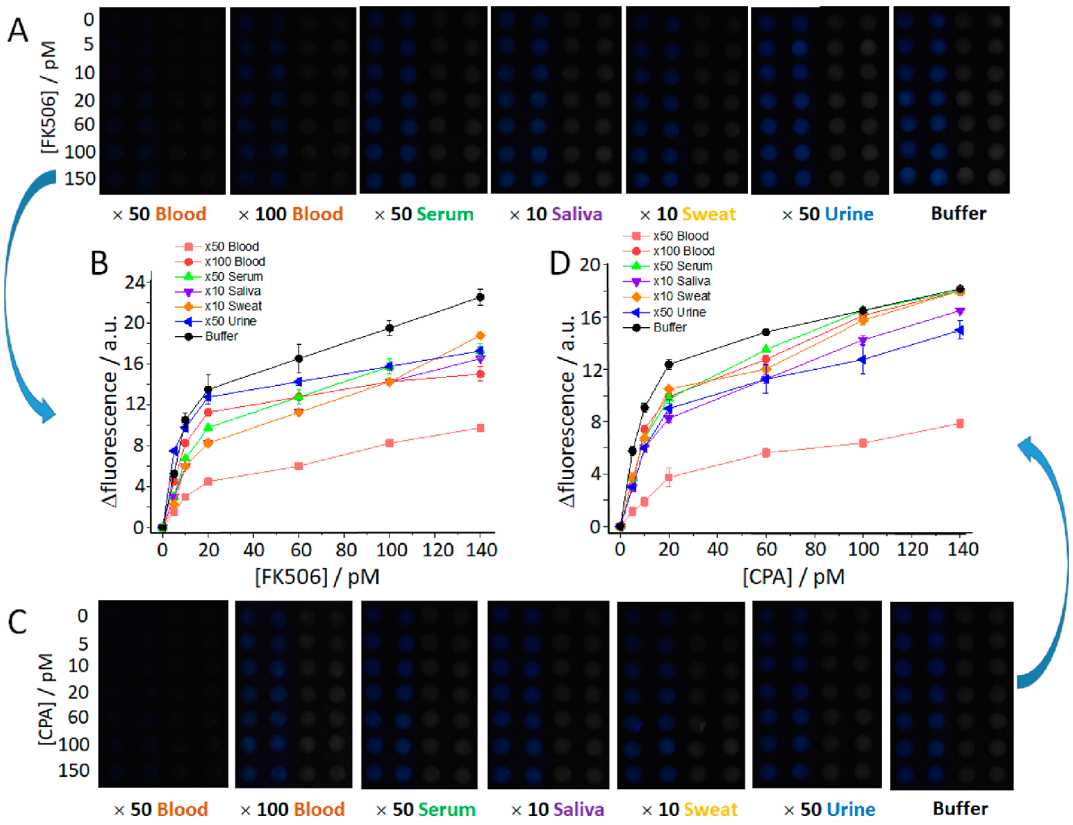

Figure 4. Detection of tacrolimus (FK506) (A) and cyclosporine A (CPA) (E) in human fluids used in different dilutions. (A) Fluorescent images (original and converted to the black-and-white format, each repeated two times) obtained for different concentrations of FK506 in biofluids using the immobilized FK506-GDH enzyme. (B) The data extracted from the images are shown in (A). (C) Fluorescent images (original and converted to the black-and-white format, each repeated two times) obtained for different concentrations of CPA in biofluids using the immobilized CPA-GDH enzyme. (D) The data extracted from the images are shown in (C).

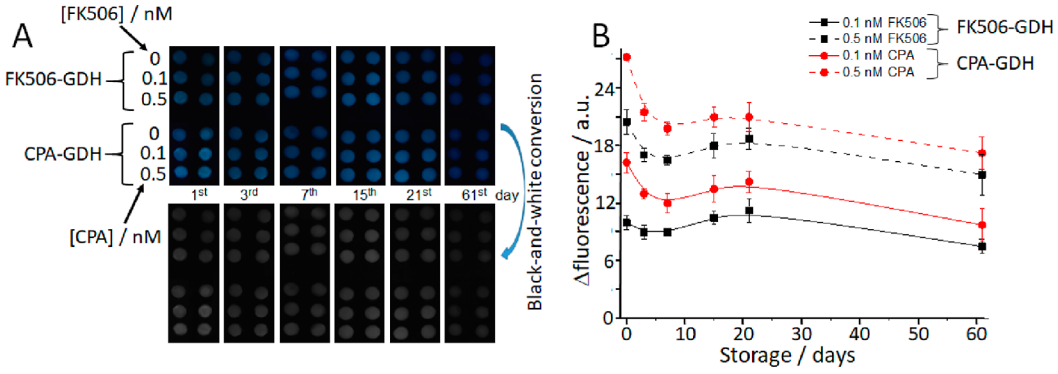

Figure 5. Long-term stability of the FK506-GDH and CPA-GDH biosensor arrays at 8 °C. (A) Fluorescent images (original and converted to the black-and-white format, each repeated two times) obtained for different concentrations of FK506 and CPA using the immobilized FK506-GDH and CPA-GDH enzymes, respectively. (B) Data extracted from the images shown in (A).

various human biofluids applied with different dilutions. The biofluids after their dilution were spiked with the drugs with different concentrations. The results clearly demonstrated that the used technique allows the analysis of the drugs in the human biofluids at their expected concentrations using a smartphone as the detection tool.

The shelf-storage stability of the biosensor array is an important factor for their potential practical utility. Figure 5 shows that the FK506-GDH and CPA-GDH biosensors (in a dry form) maintained 74 ± 1.5% and 62 ± 2.0% of their initial activity, respectively, after 2 months storage at +8 °C. Additional stability study of the biosensor, possibly at room temperature, will be needed if the biosensor commercialization is considered.

CONCLUSIONS

In the presented study, we developed an approach for the construction of biosensor arrays from single-component GDH-based protein biosensors. These biosensors were initially constructed to piggyback the glucose-monitoring technology that uses chronoamperometric detection of GDH activity to quantify blood glucose. As these biosensors contain two ligand binding domains within the same polypeptide chain, the avidity effects result in their increased affinity for the analytes.

https://doi.org/10.1021/acs.analchem.2c00650
Anal. Chem. 2022, 94, 7303−7310

Here, we tested the utility of these biosensors for the construction of optical biosensor arrays that utilize changes in fluorescence of the electron-accepting dye PMS. We demonstrate that silica nanoparticle-based arrays allow efficient and sensitive detection of the cognate analytes, such as macrocyclic drugs cyclosporine A and FK506. The apparent affinities of the biosensor for the drugs were sub-nanomolar and close to the previously determined using solution assays. However, due to the very low background, the assay displayed a remarkable dynamic range of >300-fold that is significantly larger than 4- and 10-fold dynamic ranges previously reported electrochemical or colorimetric assays, respectively.[8] This exceptional dynamic range allowed the detection of cognate ligands at concentrations significantly below the K_d with the limit of detection as low as 2 pM, which is over 20-fold improvement of previously achieved sensitivities.[8] The ability to detect such a low analyte concentration is important as it allows us to work with significantly diluted biological samples, thereby reducing the interference from sample's components. This is particularly important in the case of FK506 and cyclosporine A that must be measured in whole blood. We demonstrated that the sensory arrays can be dried down and stored for a period of months. We expect that optimization of the deposition and drying protocol make the arrays suitable for long-term storage. The only obvious drawback of the system is a relatively long incubation time required for the measurement. This can be traced back to the isomerization time of the GDH biosensors in general and requires additional biosensor analysis and optimization.[8,24] Taken together, we developed a sensitive and multiplexed bioanalytic platform that has the potential in environmental analytics as well as veterinary and human medicine.

■ ASSOCIATED CONTENT

Supporting Information

The Supporting Information is available free of charge at https://pubs.acs.org/doi/10.1021/acs.analchem.2c00650.

Additional experimental details, materials, and instrumentation and methods and figures illustrating the results discussed in the paper (PDF)

■ AUTHOR INFORMATION

Corresponding Authors

Oleh Smutok − *Department of Chemistry and Biomolecular Science, Clarkson University, Potsdam, New York 13699, United States*; Email: osmutok@clarkson.edu

Kirill Alexandrov − *CSIRO-QUT Synthetic Biology Alliance, ARC Centre of Excellence in Synthetic Biology, Centre for Agriculture and the Bioeconomy, School of Biology and Environmental Science, Queensland University of Technology, Brisbane, Queensland 4001, Australia; Bioeconomy, Centre for Genomics and Personalised Health, School of Biology and Environmental Science, Queensland University of Technology, Brisbane, Queensland 4001, Australia*; Email: kirill.alexandrov@qut.edu.au

Evgeny Katz − *Department of Chemistry and Biomolecular Science, Clarkson University, Potsdam, New York 13699, United States*; orcid.org/0000-0002-1618-4620; Email: ekatz@clarkson.edu

Authors

Paulina K. Wells − *Department of Chemistry and Biomolecular Science, Clarkson University, Potsdam, New York 13699, United States*

Zhong Guo − *CSIRO-QUT Synthetic Biology Alliance, ARC Centre of Excellence in Synthetic Biology, Centre for Agriculture and the Bioeconomy, School of Biology and Environmental Science, Queensland University of Technology, Brisbane, Queensland 4001, Australia*

Complete contact information is available at: https://pubs.acs.org/10.1021/acs.analchem.2c00650

Author Contributions

Z.G. prepared and characterized the chimeric enzymes. P.K.W. performed the main experiments with the analytical systems, processed the data, and contributed to writing the paper. O.S. performed general supervision, instructed the student, participated in the experiments, and contributed to writing of the paper. K.A. performed general supervision of synthetic biology part of the project and contributed to writing of the paper. E.K. performed general supervision of the analytical study and contributed to writing the paper.

Notes

The authors declare no competing financial interest.

■ ACKNOWLEDGMENTS

This work was supported by the Human Frontiers Science Program (HFSP) project grant RGP0002/2018 to O.S., K.A., and E.K. This work was also supported in part by the Australian Research Council Discovery Project DP150100936, as well as NHMRC grant APP1113262 to K.A. K.A. gratefully acknowledges the financial support of QUT/CSIRO Synthetic Biology alliance.

■ REFERENCES

(1) Fenton, A. W. *Trends Biochem. Sci.* **2008**, *33*, 420−425.
(2) Alberstein, R. G.; Guo, A. B.; Kortemme, T. *Curr. Opin. Struct. Biol.* **2022**, *72*, 71−78.
(3) Adamson, H.; Jeuken, L. J. C. *ACS Sens.* **2020**, *5*, 3001−3012.
(4) Makhlynets, O. V.; Raymond, E. A.; Korendovych, I. V. *Biochemistry* **2015**, *54*, 1444−1456.
(5) Nasu, Y.; Shen, Y.; Kramer, L.; Campbell, R. E. *Nat. Chem. Biol.* **2021**, *17*, 509−518.
(6) Zhou, X.; Mehta, S.; Zhang, J. *Trends Biochem. Sci.* **2020**, *45*, 889−905.
(7) Clark, J. J.; Benson, M. L.; Smith, R. D.; Carlson, H. A. *PLoS Comput. Biol.* **2019**, *15*, No. e1006705.
(8) Guo, Z.; Smutok, O.; Johnston, W. A.; Ayva, C. E.; Walden, P.; McWhinney, B.; Ungerer, J. P. J.; Melman, A.; Katz, E.; Alexandrov, K. *Angew. Chem., Int. Ed.* **2022**, *61*, No. e202109005.
(9) Guo, Z.; Parakra, R. D.; Xiong, Y.; Johnston, W. A.; Walden, P.; Edwardraja, S.; Moradi, S. V.; Ungerer, J. P. J.; Ai, H.-w.; Phillips, J. J.; Alexandrov, K. *Nat. Commun.* **2022**, *13*, 789.
(10) Liao, Z.; Wang, J.; Zhang, P.; Zhang, Y.; Miao, Y.; Gao, S.; Deng, Y.; Geng, L. *Biosens. Bioelectron.* **2018**, *121*, 272−280.
(11) Shu, J.; Tang, D. *Anal. Chem.* **2020**, *92*, 363−377.
(12) Tsai, D.; Sawyer, D.; Bradd, A.; Yuste, R.; Shepard, K. L. *Nat. Commun.* **2017**, *8*, 1802.
(13) Dincer, C.; Bruch, R.; Kling, A.; Dittrich, P. S.; Urban, G. A. *Trends Biotechnol.* **2017**, *35*, 728−742.
(14) Lv, S.; Tang, Y.; Zhang, K.; Tang, D. *Anal. Chem.* **2018**, *90*, 14121−14125.
(15) Wöhrle, J.; Krämer, S. D.; Meyer, P. A.; Rath, C.; Hügle, M.; Urban, G. A.; Roth, G. *Sci. Rep.* **2020**, *10*, 5770.

(16) Krämer, S. D.; Wöhrle, J.; Meyer, P. A.; Urban, G. A.; Roth, G. *Sci. Rep.* **2019**, *9*, 13940.
(17) Chinnadayyala, S. R.; Park, J.; Le, H. T. N.; Santhosh, M.; Kadam, A. N.; Cho, S. *Biosens. Bioelectron.* **2019**, *126*, 68−81.
(18) Xiao, Y.; Xu, L.; Qi, L.-W. *Talanta* **2017**, *165*, 577−583.
(19) Edelman, A. M.; Takio, K.; Blumenthal, D. K.; Hansen, R. S.; Walsh, K. A.; Titani, K.; Krebs, E. G. *J. Biol. Chem.* **1985**, *260*, 11275−11285.
(20) Flexer, V.; Durand, F.; Tsujimura, S.; Mano, N. *Anal. Chem.* **2011**, *83*, 5721−5727.
(21) Göbel, G.; Schubart, W.; Scherbahn, V.; Lisdat, F. *Electrochem. Commun.* **2011**, *13*, 1240−1243.
(22) Guo, Z.; Johnston, W. A.; Whitfield, J.; Walden, P.; Cui, Z.; Wijker, E.; Edwardraja, S.; Retamal Lantadilla, I.; Ely, F.; Vickers, C.; Ungerer, J. P. J.; Alexandrov, K. *J. Am. Chem. Soc.* **2019**, *141*, 8128−8135.
(23) Sallustio, B. C.; Noll, B. D.; Morris, R. G. *Clin. Biochem.* **2011**, *44*, 231−236.
(24) Edwardraja, S.; Guo, Z.; Whitfield, J.; Lantadilla, I. R.; Johnston, W. A.; Walden, P.; Vickers, C. E.; Alexandrov, K.; Vickers, C. E.; Alexandrov, K. *ACS Synth. Biol.* **2020**, *9*, 1306−1314.

https://doi.org/10.1021/acs.analchem.2c00650
Anal. Chem. 2022, 94, 7303−7310